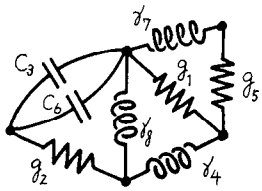


Fig. 5. Solution for Example 5.

## VI. Conclusion

It is proved that any three successive coefficients $A_k$, $A_{k+1}$, and $A_{k+2}$, when each is represented as a function of the element values, completely determine the network. This result means, for example, that the topological formula of a two-terminal impedance is uniquely determined if only any three successive coefficients of the denominator are specified as functions of the element values.

## Acknowledgment

The author wishes to thank Prof. G. Kishi, Dr. T. Kida, and A. Yamada, Tokyo Institute of Technology, for their helpful suggestions.

## References

[1] S. L. Hakimi and W. Mayeda, "On coefficients of polynomials in network functions," *IRE Trans. Circuit Theory*, vol. CT-7, Mar. 1960, pp. 40–44.
[2] S. L. Hakimi, "Graphs with two kinds of elements," *J. Franklin Inst.*, vol. 271, 1960, pp.451–467.
[3] ——, "On the realizability of a set of trees," *IRE Trans. Circuit Theory*, vol. CT-8, Mar. 1961, pp. 11–17.
[4] S. Seshu and M. B. Reed, *Linear Graphs and Electrical Networks*. Reading, Mass.: Addison-Wesley, 1961.
[5] G. Kishi and Y. Kajitani, "On realization of tree graphs," *IEEE Trans. Circuit Theory* (Corresp.), vol. CT-15, Sept. 1968, pp. 271–273.
[6] A. Chiabrera, "Properties of graphs composed of edges of two kinds," Notre Dame Conf., pp. 176–183, 1968.

# The Biquad: Part I—Some Practical Design Considerations

LEE C. THOMAS

**Abstract—The use of active elements in linear networks offers new degrees of freedom to both network and system designers. A comprehensive report on the Biquad, an active topology based on analog computer concepts, is given. We describe the electrical characteristics of the Biquad that make it a manufacturable realization for precision networks. Analysis and experimental data describe the dependence of Biquad performance on nonideal operational amplifiers. Compensation techniques are derived which allow high-Q operation at several hundred kilohertz with existing devices. The 8-V rms signal capacity and 80-dB dynamic range of the voice-frequency Biquad are illustrated.**

## I. Introduction

ACTIVE FILTER synthesis was an idea born before the technology existed to support it. A constraint common to early synthesis attempts was the need to minimize the number of active devices used. This desire was motivated by economic considerations, since gain was expensive and cost comparisons were based on the concept of a one-to-one substitution of an active device for each inductor eliminated. But minimizing the number of active devices invariably minimized the manufacturability of active filters as well. Although early studies well cataloged the reasons for the extremely sensitive networks that were implemented, their poor performance caused the engineering community generally to mistrust active networks. In fact, one might argue that the most important result of a decade of study was the development of the concept of sensitivity, about which much was written but little could be done.

The use of operational amplifiers configured as integrators, summers, and inverters for realizing linear transfer functions has remained in the bailiwick of the analog computer programmer and out of the mainstream of linear filter synthesis theory until recently [1]–[4]. The recent vigorous application of integrated circuit technology to linear active devices has considerably eased earlier economic constraints, permitting this low-sensitivity analog computer approach to compete favorably with synthesis techniques using fewer operational amplifiers.

For convenience we refer to the configuration of Fig. 1 as the Biquad, since it realizes an arbitrary biquadratic transfer function. The first-order design equations and the sensitivity of the Biquad to its passive elements are described by Tow [3]. This paper extends his description to all aspects of the electrical performance and system application of the Biquad. Specifically, we discuss minimizing sensitivity to the active element, second-order effects of finite amplifier

Manuscript received July 1, 1969; revised September 15, 1970 and October 13, 1970.
The author is with Bell Telephone Laboratories, Inc., Holmdel, N. J.

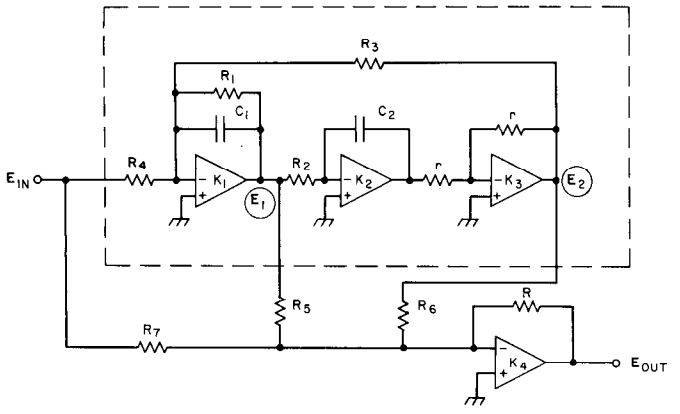


Fig. 1. Biquad circuit.

bandwidth, noise, and distortion. Experimental results are given in each case. The remainder of the paper describes the benefits which accrue from the isotopic (constant topology, variable elements) nature of the Biquad. We show that the limited concept of a block which accomplishes a filtering function and nothing more has been replaced in this case by what can be considered a multipurpose filtering system.

## II. General Description of Biquad Operation

One of the intangible attributes of the Biquad is its simplicity. In this section we describe the elements of Biquad operation. The Biquad topology is derived by generating an analog computer diagram for a biquadratic transfer function, where coefficients of the transfer function are related directly to the passive $RC$ elements which interconnect the operational amplifiers. It remains to be shown that such a derivation produces acceptably low sensitivity, but first we describe the basic operation of the Biquad. Since the topology produced by this derivation is not unique, we would expect the qualitative arguments above to apply to all topological variants.

The structure of Fig. 1 realizes a general biquadratic voltage transfer function of the form

$$\frac{E_{\text{out}}}{E_{\text{in}}} = \frac{m\left(S^2 + \frac{\omega_z}{Q_{z0}} S + \omega_z^2\right)}{S^2 + \frac{\omega_p}{Q_{p0}} S + \omega_p^2} \tag{1}$$

where $\omega_z$ and $\omega_p$ are related to the frequencies at which the loss peaks and transmission poles occur. Similarly, $Q_{z0}$ and $Q_{p0}$ are the corresponding nominal selectivities. These basic building blocks are cascaded to form transfer functions of order higher than 2. Moreover, the building block itself can be separated into recognizable submodules.

First let us consider the elements enclosed by dashed lines in Fig. 1. This part of the Biquad circuit functions independently of the rest to realize the natural modes of the system. The feedback loop consisting of $K_1$, $K_2$, and $K_3$ simultaneously realizes a bandpass ($E_1/E_{\text{in}}$) and a low-pass ($E_2/E_{\text{in}}$) transfer function with the natural modes of (1). This natural-mode circuit can be broken down still further to aid in understanding the structure. The open-loop operational amplifier $K_1$ has local feedback $R_1C_1$ and input $R_4$ to realize an inverting lossy integrator structure. Amplifier $K_2$ with its associated input $R_2$ and feedback $C_2$ is an inverting integrator. Finally $K_3$, with input and feedback $r$, is simply an inverting amplifier. The main feedback loop is closed from $K_3$ through $R_3$ to $K_1$. This structure is a simple resonator with a damping resistor $R_1$ which limits the $Q_{p0}$ of the network. The overall loop $RC$ product of such a network is the inverse of its resonant frequency squared. The inverting amplifier typically does not contribute to the loop gain, which is equally distributed between integrators $K_1$ and $K_2$, so that $\omega_p$ in (1) is given by

$$\omega_p = \frac{1}{R_3C_1} = \frac{1}{R_2C_2} \tag{2}$$

where the $RC$ products are chosen to be equal in order to minimize the sensitivity of the pole $Q$, $Q_p$, to finite operational amplifier gain [2]. For this case, where the $RC$ product of the first integrator $K_1$, $(1/R_3C_1)$ is the same as that of the second integrator $K_2$, $(1/R_2C_2)$, the $Q_{p0}$ of the transmission poles is given by

$$Q_{p0} = R_1/R_3. \tag{3}$$

Thus $R_1$ directly determines the $Q_{p0}$ of the Biquad and $R_2$ or $R_3$ may be used to adjust $\omega_p$. The voltage gain at resonance $\omega_p$ is independently determined by the input resistor $R_4$ in

$$G = \left.\frac{E_1}{E_{\text{in}}}\right|_{\omega_p} = \left.\frac{E_2}{E_{\text{in}}}\right|_{\omega_p} = \frac{R_1}{R_4}. \tag{4}$$

Notice that this natural mode structure is inherently stable ($Q_{p0}$ is always positive for $R_1$ and $R_3 > 0$). In addition, the structure has a low output impedance and a high-impedance purely resistive input. Inspection will show that a weighted sum of $E_{\text{in}}$, $E_1$, and $E_2$ will produce an arbitrary quadratic numerator, completing the desired biquadratic transfer function. Complete details of the synthesis equations may be found in [3] and [5]. The next section discusses the electrical performance of the network of Fig. 1.

## III. Electrical Performance of the Biquad

Comparing the relative merits of the many available active synthesis techniques is a nontrivial task. In this section we introduce the concept of *precision*, which has proved a useful addition to the sensitivity concept in evaluating overall performance. It is demonstrated that the precision of the Biquad is comparable to the passive case. Also, as the resonant frequency of the Biquad is increased, the $Q_{p0}$ given by (3) does not equal the *actual* $Q_p$ of the network. The actual $Q_p$ increases at high resonant frequencies because of finite gain and bandwidth effects in the nonideal operational amplifiers. Analysis and supporting data are presented which allow the $Q_p$ versus resonant frequency characteristic of the Biquad to be predicted as a function of the gain and bandwidth of the amplifier. Finally we discuss data on tuning, temperature dependence, noise, distortion, and signal

level which illustrate the overall performance to be expected from today's active devices.

*Biquad Sensitivity*

The sensitivities of various aspects of performance to parameter variation have proved useful concepts in evaluating active synthesis techniques. Tow [3] has shown that the sensitivity of the natural modes of the Biquad to its passive elements is comparable to the passive $LC$ case, a fact which yields precision performance and simple tuning. The crucial sensitivity for active realization is the sensitivity of the actual natural mode $Q_p$ to the active element, in this case the finite open-loop gain of the operational amplifier $\mu_0$. This sensitivity is defined as

$$S_{\mu_0}^{Q_p} = \frac{\mu_0}{Q_p}\frac{dQ_p}{d\mu_0}. \tag{5}$$

For a finite-gain infinite-bandwidth amplifier, (43) [see Appendix I] gives

$$Q_p = \frac{Q_{p0}}{1 + \dfrac{2Q_{p0}}{\mu_0}} \tag{6}$$

where $Q_{p0}$ is the nominal $Q_p$ of (3) and $\mu_0$ is the open-loop gain of $K_1$ and $K_2$. Thus, from (5) and (6)

$$S_{\mu_0}^{Q_p} = \frac{2Q_p}{\mu_0}. \tag{7}$$

In most passive realizations of interest, the sensitivities of all relevant transfer characteristics ($\omega_p$, $Q_p$, etc.) to passive components are less than or equal to unity. For precision applications, the component tolerance is usually about 1 percent. This means that a 1-percent component error will result in a 1-percent error in the transfer function coefficients, at worst. The total picture, then, is reflected by the inverse sensitivity–variability product, or precision $P$, of the network, which we require to be greater than unity with the variability $V$ measured in percent. Adopting the passive case as a standard, we require $P > 1$. For example,

$$P_{\mu_0}^{Q} = \frac{1}{S_{\mu_0}^{Q} V_{\mu_0}} \geq 1. \tag{8}$$

From (7) the precision of the Biquad for $V_{\mu_0}$ equal to 50 percent is given by

$$P_{\mu_0}^{Q_p} = \frac{\mu_0}{100\, Q_p} \geq 1. \tag{9}$$

Thus, very high precision realizations can be obtained with a Biquad for $\mu_0 \geq 100\ Q_p$. More reasonable requirements, yielding a maximum 5-percent change in $Q_p$, would call for $\mu_0 \geq 20\ Q_p$.

*$Q_p$ Enhancement Caused by Finite Gain-Bandwidth*

The preceding section discusses the high-precision, high-$Q_p$ limitations of the Biquad for the case of finite amplifier gain. This section develops the limits imposed by the finite bandwidth of the amplifier. Fig. 2 shows experimental and analytic curves of the actual $Q_p$ of the Biquad as a function of the resonant frequency $\omega_p$. The design value $Q_{p0} = R_1/R_3$ is held constant as $\omega_p$ is varied with $C_1$ and $C_2$. Note that after remaining constant over a broad band, the $Q_p$ begins to increase and then becomes infinite (unstable). Such an increase in $Q_p$ is called $Q_p$ enhancement. Appendix I presents an analysis of the $Q_p$ enhancement effect assuming a finite-bandwidth amplifier of the form

$$\mu = \frac{\mu_0\omega_a}{S + \omega_a}. \tag{10}$$

From (44) [see Appendix I]

$$Q_p = \frac{Q_{p0}}{1 + \dfrac{2Q_{p0}}{\mu_0\omega_a}(\omega_a - 2\omega_p)}. \tag{11}$$

Thus, as we attempt to reach higher values of $\omega_p$ for constant $Q_{p0}$, $\mu_0$, and $\omega_a$, the denominator of (11) goes to zero. The match between (11) and the experimental measurements given in Fig. 2 is obtained by using values in (11) for $\mu_0$ and $\omega_a$ that are determined from independent measurements of the amplifier in question. The 709 curves shown in Fig. 2 are based on $\mu_0 = 33\,000$ and $f_a = 1200$ Hz. The 1T is a Western Electric amplifier similar to the 702 but having higher frequency transistors. These curves, shown in Fig. 2, are based on $\mu_0 = 3000$ and $f_a = 20$ kHz. The very high gain-bandwidth products for these two amplifiers are obtained by using a very light frequency compensation on each amplifier. (The compensation used for the 709 TO-99 package is 2700 Ω in series with 100 pF from pin 1 to pin 8 and 82 pF from pin 5 to pin 6. The 1T is compensated by 25-pF lead compensation and 100 Ω in series with 25 pF as lag compensation.) The Biquad topology is particularly suitable for such light compensation because, basically, an integrator is a compensated operational amplifier having leading phase feedback at high frequencies. That is, the feedback capacitors which perform the integrating function also provide loop gain and phase shaping to stabilize the amplifier. Such an arrangement allows higher frequency operation for a given amplifier than most structures.

On the basis of (40), we can conclude that the introduction of *leading* phase to cancel the lagging phase introduced by the finite amplifier bandwidth should extend the point at which $Q_p$ enhancement occurs. In the topology of Fig. 1, leading phase can be introduced by placing a small capacitance $C_c$ across $R_2$ or $R_3$. The data of Fig. 2 include the effect of $C_c = 3$ pF across $R_3 = 4$ kΩ. Substituting the measured values of $\mu_0$ and $\omega_a$ in (47) yields $C_c = 2.65$ pF, an excellent agreement. The limiting factor with this phase-cancellation technique results from the finite slew rate of the amplifiers. As we attempt to extend the maximum operating frequency indefinitely, the structure becomes conditionally stable. At low signal levels the circuit is stable and the $Q_p$ is not enhanced. As the level is raised, however, slew-rate limiting occurs, introducing an equivalent lagging phase which

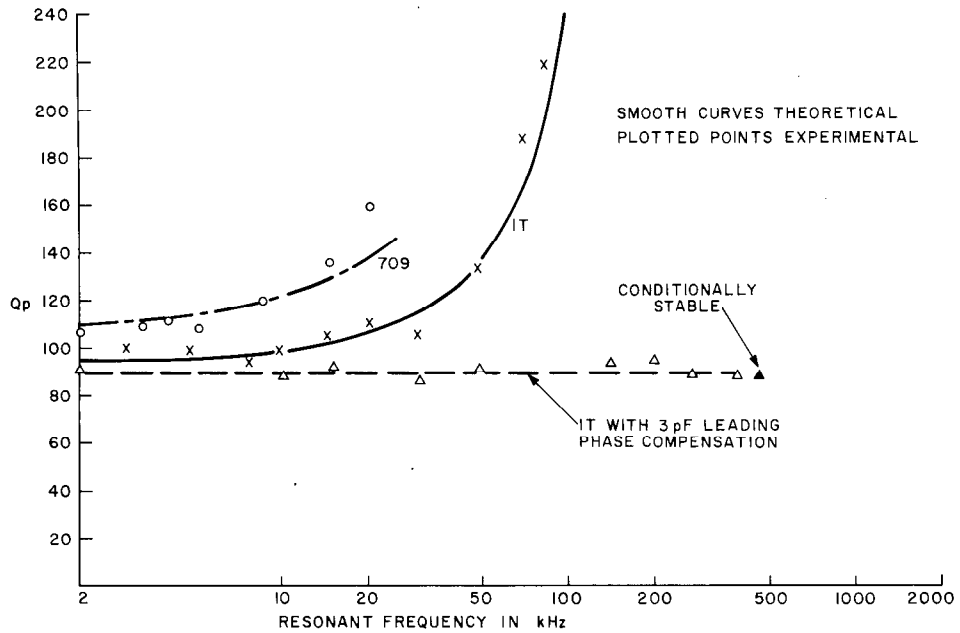


Fig. 2. Actual $Q_p$ of Biquad section as function of resonant frequency $f_p$ for constant nominal $Q_{p0}$.

causes oscillation at $\omega_p$. This source of oscillation is therefore a nonlinear dependence of amplifier phase lag on the rate of change of the output voltage.

*Noise, Distortion, and Signal Level*

While passive networks, particularly those employing toroidal inductors, are not without distortion problems, our concern about nonlinear effects tends to be greater with active networks. Also, active elements introduce noise which must be considered in meeting system specifications. Using the 709, a single Biquad section has a broad-band output noise level less than 100 $\mu$V rms, independent of the net gain of the section. As sections are cascaded, the total noise adds on a power basis. If signal voltages are large (8 V rms) a unity-gain filter will provide an excellent signal-to-noise ratio. However, if the signal level is low (100 $\mu$V rms), we can introduce gain in the filter to boost the output signal without affecting the output noise level. In essence, then, a Biquad filter section can provide its own low-noise preamplification simply by adjusting the gain-determining resistor $R_4$. This example of preamplification and filtering in the same block illustrates the multipurpose nature of the Biquad. The penalty for introducing gain into a Biquad section is usually acceptable. When the gain $G$ is not negligible with respect to the $Q_p$, from (42)

$$S_{\mu_0}^{Q_p} = \frac{2}{\mu_0}\left(Q_p + \frac{G}{2}\right). \tag{12}$$

Thus, the equivalent $Q_p$ of a section, for sensitivity purposes, is the actual $Q_p$ plus half the gain. For example, a section with a gain of 40 dB and a $Q_p$ of 100 has the same sensitivity (and precision) as a low-gain section with $Q_p = 150$. In a multisection filter the gain can be distributed among the sections, but for maximum signal-to-noise improvement most of the gain should, of course, be in the first section.

The distortion performance of the Biquad provides a dynamic range consistent with its large signal-to-noise ratio. The Biquad has a sharply breaking distortion characteristic typical of feedback amplifiers. Allowing maximum second-harmonic distortion 80 dB below the fundamental, the 709 can handle signals of 11 V peak and the 1T has a peak limit of about 2.5 V. These peak signals and the noise-distortion floor indicate that a Biquad has about 80-dB dynamic range. Using the preamplification techniques mentioned above, the full dynamic range can be utilized in any application. In severe cases, obtaining the full dynamic range in a multisection filter requires judicious pole-zero pairing and sequencing of sections, considerations beyond the scope of this paper. As a final comparison, passive network designers will be aware that the signal levels quoted here are much greater than those normally used in low-frequency passive networks utilizing toroidal inductors.

*Noninverting Integrators*

In most applications it is possible to dispense with the inverting amplifier $K_3$ of Fig. 1 by using a noninverting integrator configuration in place of the second inverting Miller integrator $K_2$. Two such integrators are shown: the balanced time-constant (BTC) integrator in Fig. 3(a), and the resistance-bridge (RB) integrator in Fig. 3(b). The price one pays for eliminating an amplifier and its power consumption is an extra tuning step and increased sensitivity to the passive elements in the noninverting integrator. As operational amplifier prices continue to decrease, the cost of this extra step will have to be weighed against the cost of the amplifier, but in the meantime the noninverting integrator offers significant economies.

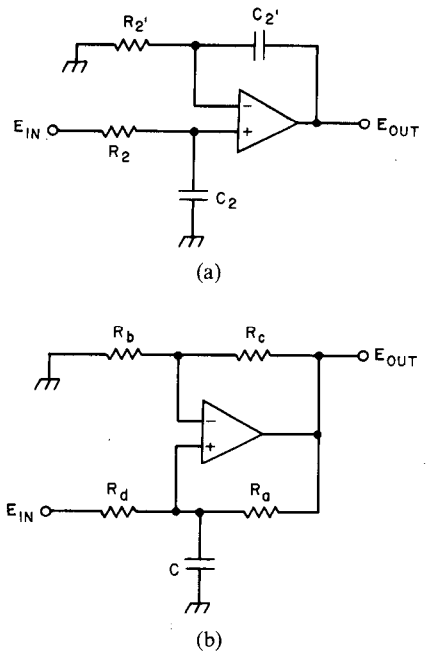


Fig. 3. Two noninverting integrator configurations. (a) BTC integrator. (b) RB integrator.

As shown in Appendix II, the BTC integrator is a perfect integrator only when $R_2C_2 = R_2'C_2'$. The effect on $Q_p$ of an imbalance in these time constants is given by [see Appendix II, (53)]:

$$Q_p = \frac{Q_{p0}}{1 + \frac{Q_{p0}}{2}\left[\frac{R_2'C_2'}{R_2C_2} - 1\right]}. \tag{13}$$

The correlation between (13) and measured results is shown in Fig. 4.

The BTC integrator is tuned by lifting $R_2'$ off and driving $R_2$ and $R_2'$ with a common source at $\omega_p$. Such an arrangement requires that dc be injected to balance the offset voltages that occur with this arrangement. On an ac basis the transfer function of this structure, evaluated at $\omega_p$, is given by

$$|T(j\omega_p)| \simeq \frac{1}{\sqrt{2}}\left[\frac{R_2'C_2'}{R_2C_2} - 1\right]. \tag{14}$$

Equation (13) indicates that we desire a null in $T(j\omega_p)$ for $Q_p = Q_{p0}$. The required depth of the null for a known error in $Q_p$ can be derived by comparing (13) and (14). From (13) define the error $\varepsilon_Q$ as

$$\varepsilon_Q = \tfrac{1}{2}Q_{p0}\left[\frac{R_2'C_2'}{R_2C_2} - 1\right]. \tag{15}$$

Then

$$|T(j\omega_p)| = \frac{\sqrt{2}\varepsilon_Q}{Q_{p0}}. \tag{16}$$

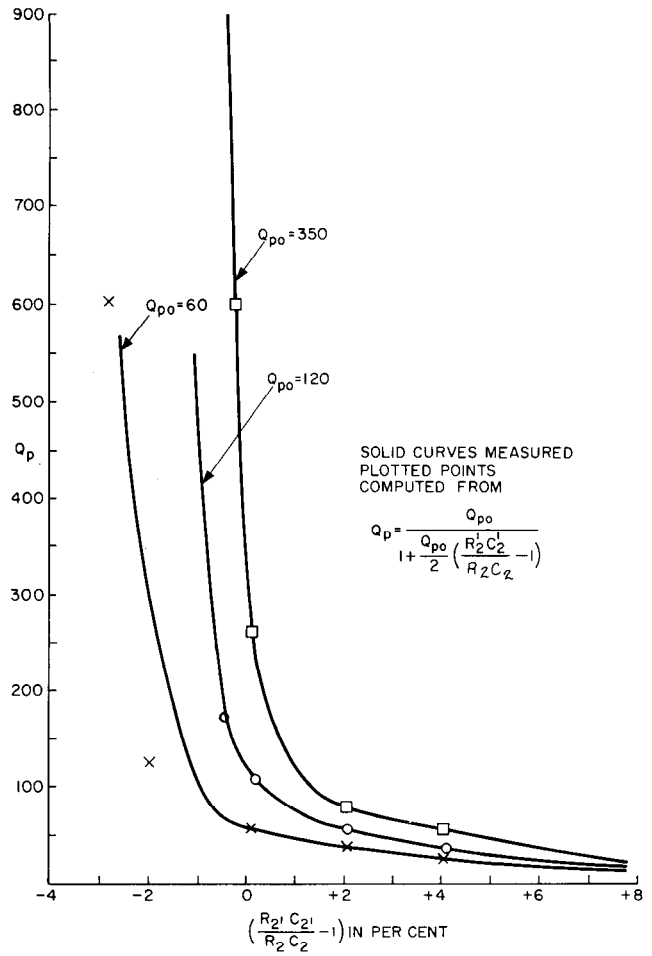


Fig. 4. Actual $Q_p$ of Biquad Section as function of $R_2'C_2'$, $R_2C_2$ imbalance.

For example, for $Q_{p0} = 100$ and $\varepsilon_Q = 0.01$, we would seek a 77-dB null in $T(j\omega_p)$ by adjusting $R_2$. An indication of the critical nature of this adjustment can be obtained by computing the sensitivity of $Q_p$ to the ratio $R_2'C_2'/R_2C_2$. From (13), for $\mathscr{R} = [R_2'C_2'/R_2C_2] \approx 1$,

$$S_{\mathscr{R}}^{Q} \simeq -\tfrac{1}{2}Q_p. \tag{17}$$

Equation (17) is an elaboration on the impression given by Fig. 4. For high $Q_p$ the sensitivity to time constant imbalance is large. However, as a practical matter, tracking of the components with temperature greatly reduces the net effect, as demonstrated in the section on temperature effects.

In the case of the RB integrator of Fig. 3(b), a similar analysis holds. Define the ratio

$$\frac{R_cR_d}{R_aR_b} = \rho. \tag{18}$$

Then, from Appendix II, (61), we find

$$Q_p = \frac{Q_{p0}}{1 + Q_{p0}(1 - \rho)} \tag{19}$$

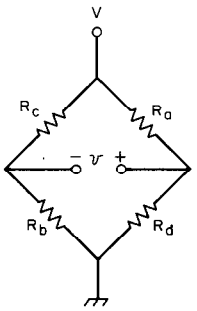


Fig. 5. Dc bridge balancing arrangement for RB integrator.

indicating that for ideal operation of the RB integrator we desire $\rho = 1$. The error in $Q_p$, $\bar{\varepsilon}_Q$ is given by

$$\bar{\varepsilon}_Q = Q_{p0}(1 - \rho). \tag{20}$$

The RB integrator can be tuned on a dc basis. Omitting the operational amplifier and grounding $R_d$ yields a resistance bridge, as shown in Fig. 5. The bridge balance equation is given by

$$v = \tfrac{1}{4}V(1 - \rho) \tag{21}$$

indicating a desired bridge null for a given $\bar{\varepsilon}_Q$ of

$$\frac{v}{V} = \frac{\bar{\varepsilon}_Q}{4Q_{p0}}. \tag{22}$$

Using the same example as before, $\bar{\varepsilon}_Q = 0.01$ and $Q_{p0} = 100$ indicate a desired null of 92 dB on a dc basis. As in the case of the BTC integrator, our sensitivity to passive elements is again proportional to the $Q_p$. From (19) for $\rho \approx 1$,

$$S_\rho^{Q_p} \simeq -Q_p. \tag{23}$$

*Temperature Effects*

Because of its very low sensitivity to the highly variable active element, the temperature stability of the Biquad is dependent only on the passive components. Drift in $\omega_p$ is usually a prime consideration. This drift is minimized when the capacitor temperature coefficients of $C_1$ and $C_2$ are equal and opposite to the resistor temperature coefficients of $R_2$ and $R_3$. A mismatch of 200 ppm/°C will yield a worst case shift in $\omega_p$ of 1 percent over a 50°C range. Such a shift would be tolerable only in applications with percentage bandwidths greater than 5 percent or 10 percent. About the best $RC$ match that can reasonably be obtained is 20 ppm/°C, yielding a 0.1-percent shift in $\omega_p$. Therefore, on the basis of passive element stability, a useful upper limit on active network $Q$ operating over a 50°C range would be on the order of 200. If higher $Q_p$ is desired, the more stable mechanical resonators should be considered or the environment must be controlled.

*Summary of Electrical Performance*

We have presented analytic and experimental confirmation of the Biquad's performance as a highly stable manufacturable network. Stable low-sensitivity $Q_p$ of several hundred can be obtained up to 10 kHz for the 709 operational amplifier. The maximum useful $Q_p$ obtainable with the Western Electric 1T is about 100, but this selectivity can be achieved at 400 kHz. Maximum voltage levels of 8 V rms and a noise floor less than 100 $\mu$V give versions utilizing the 709 a signal-to-noise ratio of about 80 dB. The 1T offers a maximum voltage of about 1.8 V rms and a dynamic range of about 80 dB. Because of its low sensitivity to passive elements, tuning the Biquad is a simple noninteractive process. The stability of the resonant frequency with temperature is strictly a function of the stability of an $RC$ product. An important variation of the Biquad topology uses a noninverting integrator structure which saves one operational amplifier per section at the expense of a more complex tuning process and increased sensitivity to passive components.

## Appendix I

The purpose of this appendix is to establish the analytic relationship between the natural mode $Q_p$ of the Biquad and the first- and second-order parameters of the passive and active components.

We begin by observing that $Q_p$ may be expressed in terms of the phase *lag* at resonance around the major feedback loop of Fig. 1. For ideal $K_1$, $K_2$, and $K_3$, it is simple to derive the relation

$$\frac{E_1}{E_{\text{in}}} = -\frac{1}{R_4C_1}\,\frac{S}{S^2 + \dfrac{1}{R_1C_1}S + \dfrac{1}{R_2C_2R_3C_1}}. \tag{24}$$

Relating the terms of (24) to the standard form of a second-order system, we identify the bandwidth $\Delta\omega$:

$$\Delta\omega = 1/R_1C_1 \tag{25}$$

and the resonant frequency $\omega_p$:

$$\omega_p = \sqrt{1/R_2C_2R_3C_1}. \tag{26}$$

For ideal amplifiers the closed-loop transfer function of the first integrator $K_1$ is

$$T_1(S) = \frac{-1}{R_3C_1}\,\frac{1}{S + \Delta\omega}. \tag{27}$$

Thus the phase lag of $K_1$ at resonance $\omega_p$ is

$$\Phi_1 = \pi/2 - \tan^{-1}\frac{\Delta\omega}{\omega_p}. \tag{28}$$

For $Q_{p0} > 10$ or $\omega_p/\Delta\omega > 10$, we can approximate (28) by

$$\Phi_1 \simeq \pi/2 - \Delta\omega/\omega_p = \pi/2 - 1/Q_{p0}. \tag{29}$$

The lagging phases of the second integrator and the inverter are simply

$$\Phi_2 = \pi/2 \tag{30}$$

and

$$\Phi_3 = \pi \tag{31}$$

respectively. Thus the net phase lag around the loop is approximately

$$\Phi_T = \Phi_1 + \Phi_2 + \Phi_3 \simeq -1/Q_{p0}. \tag{32}$$

For the nonideal case, where our amplifiers have open-loop gains of the form

$$\mu = \frac{\mu_0\omega_a}{S + \omega_a} \tag{33}$$

we obtain

$$T_1(S) \simeq \frac{-\mu_0\omega_a\omega_p}{S^2 + S(\mu_0\omega_a) + \omega_a\left(\mu_0\Delta\omega + \omega_p + \dfrac{G\omega_p}{Q_{p0}}\right)} \tag{34}$$

for $\mu_0 \gg 1$ and $\omega_p/\Delta\omega \gg 1$, where $G$ is the gain $R_1/R_4$ from (6).

Similarly, for the second integrator $K_2$,

$$T_2(S) = \frac{-\mu_0\omega_a\omega_p}{S^2 + (\mu_0\omega_a)S + \omega_a\omega_p} \tag{35}$$

and for the inverter $K_3$,

$$T_3(S) = -\frac{1}{2}\frac{\mu_0\omega_a}{S + \mu_0\omega_a/2}. \tag{36}$$

From (34)–(36) we obtain for $S = j\omega_p$,

$$\Phi_1 \simeq \pi/2 - 1/Q_{p0} - 1/\mu_0 + \omega_p/\mu_0\omega_a - G/Q_{p0}\mu_0 \tag{37}$$

$$\Phi_2 \simeq \pi/2 - 1/\mu_0 + \omega_p/\mu_0\omega_a \tag{38}$$

$$\Phi_3 \simeq \pi + 2\omega_p/\mu_0\omega_a. \tag{39}$$

Now, assuming (32) holds for small perturbations of the loop phase around the nominal,

$$\Phi_T \simeq -1/Q_p \simeq -1/Q_{p0} - 2/\mu_0 + 4\omega_p/\mu_0\omega_a - G/Q_{p0}\mu_0 \tag{40}$$

or

$$Q_p = \frac{Q_{p0}}{1 + \dfrac{2Q_{p0}}{\mu_0}\left[1 - 2\left(\dfrac{\omega_p}{\omega_a}\right)\right] + \dfrac{G}{\mu_0}}. \tag{41}$$

Alternate forms of (41) are obtained for $\omega_a \to \infty$:

$$Q_p = \frac{Q_{p0}}{1 + \dfrac{2Q_{p0} + G}{\mu_0}} \tag{42}$$

and when the gain at resonance $G \ll 2Q_{p0}$,

$$Q_p = \frac{Q_{p0}}{1 + \dfrac{2Q_{p0}}{\mu_0}}. \tag{43}$$

In terms of the gain-bandwidth product $\mu_0\omega_a$, for $G \ll 2Q_{p0}$,

$$Q_p = \frac{Q_{p0}}{1 + \dfrac{2Q_{p0}}{\mu_0\omega_a}(\omega_a - 2\omega_p)}. \tag{44}$$

Observe that we can totally eliminate (to the extent that our approximations are correct) the dependence of $Q_p$ on $\omega_p$ by canceling the term $4\omega_p/\mu_0\omega_a$ in (40) with an additional *leading* phase component. Such a phase term can be introduced by placing a small compensating capacitor $C_c$ in parallel with one of the loop resistances, say $R_3$. The lagging phase $\phi_c$ of such a component is given by

$$\phi_c \simeq -\omega_p R_3 C_c. \tag{45}$$

Then we require $\phi_c$ to subtract from $\Phi_T$ of (40) an amount

$$\phi_c = -4\omega_p/\mu_0\omega_a - \omega_p R_3 C_c. \tag{46}$$

Then

$$C_c = \frac{4}{\mu_0\omega_a R_3}. \tag{47}$$

## Appendix II

The transfer function of the BTC integrator of Fig. 3(a) is given by

$$\frac{E_{out}}{E_{in}} = \frac{1}{SR_2C_2}\left[\frac{S + \dfrac{1}{R_2'C_2'}}{S + \dfrac{1}{R_2C_2}}\right]. \tag{48}$$

Thus, this structure depends on a pole-zero cancellation, effected by balancing $R_2C_2 = R_2'C_2'$, to yield a perfect integrator. The $Q$ degradation introduced by an imbalance in these time constants can be derived from the principle of (32): the total phase lag around the loop is the negative reciprocal of the $Q_p$ of the network. Evaluating (48) at $S = j\omega_p = 1/R_2C_2$:

$$\frac{E_{out}}{E_{in}} = \frac{1}{j}\left[\frac{j\dfrac{1}{R_2C_2} + \dfrac{1}{R_2'C_2'}}{j\dfrac{1}{R_2C_2} + \dfrac{1}{R_2C_2}}\right]. \tag{49}$$

This phase lag deviates from the desired $-\pi/2$ by

$$\phi_\varepsilon = -\tan^{-1}\frac{R_2'C_2'}{R_2C_2} + \tan^{-1} 1. \tag{50}$$

For $R_2'C_2'/R_2C_2$ near unity,

$$\phi_\varepsilon \simeq -\frac{1}{2}\left[\frac{R_2'C_2'}{R_2C_2} - 1\right]. \tag{51}$$

Assuming no other degradations, then the degraded $Q_p$ is derived from

$$\frac{1}{Q_p} = -\Phi_T = \frac{1}{Q_{p0}} - \phi_\varepsilon = \frac{1}{Q_{p0}} + \frac{1}{2}\left[\frac{R_2'C_2'}{R_2C_2} - 1\right] \tag{52}$$

or

$$Q_p = \frac{Q'_{p0}}{1 + \frac{Q_{p0}}{2}\left[\frac{R'_2C'_2}{R_2C_2} - 1\right]}. \tag{53}$$

The transfer function of the RB integrator of Fig. 3(b) is given by

$$\frac{E_{\text{out}}}{E_{\text{in}}} = \frac{1 + \frac{R_c}{R_b}}{SR_dC + 1 - \frac{R_cR_d}{R_dR_b}}. \tag{54}$$

For convenience in computing the phase error $\bar{\phi}_\varepsilon$ introduced by the RB integrator at $S=j\omega_p$, we take

$$R_c/R_b \simeq 1 \tag{55}$$

$$\omega_p \simeq 1/R_dC \tag{56}$$

and

$$\frac{R_cR_d}{R_aR_b} \triangleq \rho. \tag{57}$$

Then

$$\left.\frac{E_{\text{out}}}{E_{\text{in}}}\right|_{j\omega_p} \simeq \frac{2}{1 - \rho + j1} \tag{58}$$

and the lag error is

$$\bar{\phi}_\varepsilon = -\tan^{-1}(1 - \rho) \simeq -(1 - \rho) \tag{59}$$

for $\rho$ near unity. Using our reciprocal relation between $\Phi_T$ and $Q_p$, we obtain

$$\frac{1}{Q_p} = \frac{1}{Q_{p0}} - \bar{\phi}_\varepsilon = \frac{1}{Q_{p0}} + 1 - \rho \tag{60}$$

or

$$Q_p = \frac{Q_{p0}}{1 + Q_{p0}(1 - \rho)}. \tag{61}$$

## ACKNOWLEDGMENT

The contents of this paper represent a selection of the results of a year of intensive development involving many people. The theoretical results are distilled from the ideas and efforts of several people and cannot be considered the unique contribution of the author. The author particularly wishes to thank C. F. Simone and E. J. Angelo, Jr., whose daily interaction on all phases of the development has been a source of progress and enjoyment, and C. N. Tanga and R. L. Ukeiley, by whom a significant portion of the experimental data presented here was obtained.

## REFERENCES

[1] W. J. Kerwin, L. P. Huelsman, and R. W. Newcomb, "State-variable synthesis for insensitive integrated circuit transfer functions," *IEEE J. Solid-State Circuits*, vol. SC-2, Sept. 1967, pp. 87–92.

[2] A. J. L. Muir and A. E. Robinson, "Design of active RC filters using operational amplifiers," *Syst. Technol.*, Apr. 1968, pp. 18–30.

[3] J. Tow, "Active RC filters—A state-space realization," *Proc. IEEE* (Lett.), vol. 56, June 1968, pp. 1137–1139.

[4] G. Hurtig, "Positive results from negative feedback," *Electronics*, Mar. 31, 1969, pp. 96–102.

[5] J. Tow, "A step-by-step active filter design," *IEEE Spectrum*, vol. 6, Dec. 1969, pp. 64–68.